COMPUTATION OF PARAMETERS IN NMR USING INTEGRAL TRANSFORMS: TAPERED AREAS

Fred K. Gruber, Lalitha Venkataramanan, Denise E. Freed, and Tarek M. Habashy

Schlumberger-Doll Research Center, One Hampshire Street, Cambridge, MA 02139, USA

ABSTRACT

This paper describes a method to compute tapered areas of a probability density function by means of integral transforms of its noisy Laplace transform. This problem is directly relevant to Nuclear Magnetic Resonance data for fluid and rock characterization. We describe integral transforms that are directly applicable to the measured magnetisation data, to estimate the tapered areas. In petrophysics, these tapered areas are useful in estimation of fluid saturations and bound and free fluid volumes. Since integral transforms are linear, uncertainty in the tapered areas can be computed as a function of signal-to-noise (SNR) in the data. Performance of these transforms is demonstrated on simulated data and compared to results from the traditional inverse Laplace transform.

Index Terms— Inverse Laplace transform, Nuclear Magnetic Resonance, analysis of exponentially decaying data, petrophysics

1. INTRODUCTION

The acquired magnetization decay in Nuclear Magnetic Resonance (NMR) experiments is commonly modeled by a sum-of-exponentials model that relates the measurements $M(t)$ with a Laplace transform of the underlying probability density function $f_{T_2}(T_2)$, also known as T_2 distribution, such that

$$M(t) = \int_0^\infty e^{-\frac{t}{T_2}} f_{T_2}(T_2) dT_2 + \epsilon(t) \qquad (1)$$

where $\epsilon(t)$ denotes the additive white, Gaussian noise with known statistics.

In many applications, the parameters of interest correspond to specific areas of the density distribution. As shown in Fig. 1, these areas are often found using either sharp or tapered cut Heaviside functions in $\log(T_2)$ domain [1].

In oilfield applications, $f_{T_2}(T_2)$ is often considered to directly reflect the rock-pore size distribution with short relaxation times T_2 corresponding to small pores and larger relaxation times corresponding to larger pores. Thus, in these applications, sharp or tapered areas of $f_{T_2}(T_2)$ are often thought to directly provide information of underlying pore geometry.

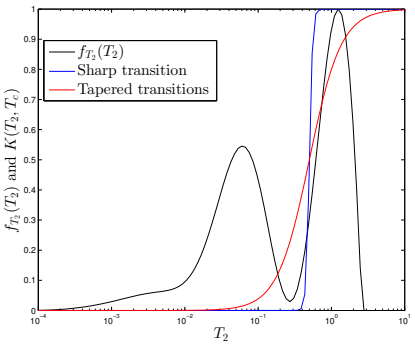

Fig. 1. Tapered vs. sharp areas.

Although sharp transitions are routinely used to compute areas, tapered transitions have recently been considered to reflect better the underlying physics of NMR relaxation and capillary pressure of fluids in rocks [2]. Sharp and tapered areas have many applications including the following:

1. Computation of discrete pore sizes: In complex carbonate rock, the T_2 distribution is often discretized into three distinct bins, reflecting the three different pore-sizes - micro, meso and macro-pores. Inferences from this discretization have been used with other data sets to help understand relationships between the geological facies and petrophysical and reservoir-flow properties of these complex carbonate rocks.

2. Separation of bound and free fluid: Since $f_{T_2}(T_2)$ is thought to reflect the pore size distribution, bound and free fluid volumes are often determined by applying a sharp cut-off to the T_2 distribution. Based on lab experiments, areas above the cut-off is related to the free fluid volume indicating large pores potentially capable of producing and area below the cut-off is related to bound fluid volume indicating small pores containing fluid that is trapped by capillary pressure and incapable of producing fluid[3].

3. Computation of hydrocarbon and water saturations: When two distinct peaks are seen in T_2 distributions,

one of them is often associated with the water phase while the other is associated with hydrocarbon. The position of the oil peak as well as the area underneath is used to estimate hydrocarbon viscosity and saturation respectively [3].

2. RELATION TO PRIOR WORK

Traditionally, the sharp or tapered areas are computed as follows. An inverse Laplace transform (ILT) algorithm is used to estimate $f_{T_2}(T_2)$ from the measured $M(t)$ (see [4] and references therein). Petro-physical parameters such as fluid saturations or bound and free fluid volumes are computed from either sharp or tapered areas obtained from the T_2 distribution. Since T_2 spans decades from milli-seconds to seconds, the tapered areas are computed in $\log(T_2)$ domain. However, it is well-known that the ILT is an ill-conditioned problem requiring regularization and incorporation of prior information about the solution into the problem formulation [5, 6]. Due to their non-uniqueness, the choice of the regularization functional as well as the weight given to prior information are well-known drawbacks of ILT algorithm

In this paper, we describe a method based on integral transforms to directly provide tapered areas. This method obviates the need to compute $f_{T_2}(T_2)$ using the ill-conditioned ILT. An important aspect of this work is that it helps quantify parameters that can be reliably obtained from the data and their dependence on the signal to noise ratio (SNR) in the data. This integral transform method to estimate areas can be generalized to multiple dimensions such as other NMR modalities like diffusion-relaxation and $T_1 - T_2$ data [7].

Section 3 of this paper describes a few simple integral transforms such as the sinc, exponential Haar and exponential sine transforms to compute tapered areas as well as some ideas to deal with sharper transitions. Section 4 compares simulation results from the integral transform method with results from the traditional ILT. Finally, section 5 concludes this paper.

3. TAPERED TRANSITIONS IN $\log(T_2)$ DOMAIN

An integral transform of the measured data is defined as

$$K\left[M(u)\right] \equiv \int_0^\infty k(t,u)M(t)dt \tag{2}$$

The integral transform is specified by its kernel function $k(t,u)$. Examples of often-used integral operators include Laplace, Fourier and Hankel transforms. In our application, when the data is described by eqn. (1), we have previously shown that when the kernel is the Mellin operator where the kernel of the integral equation is given by $k(t,u) = \frac{t^{u-1}}{\Gamma(u)}$, eqn. (2) directly provides moments of T_2 relaxation time [8].

Here, we describe several kernels $K\left[M(u)\right]$ such that eqn. (2) directly provides tapered areas in the specified T_2 region. As shown in Fig. 1, let T_c denote the T_2 relaxation time at which the desired cut-off is 0.5. The tapered area is,

$$A = \int_0^\infty k(t,T_c)M(t)dt \tag{3}$$

$$= \int_0^\infty K(T_2,T_c)f_{T_2}(T_2)dT_2. \tag{4}$$

where $K(T_2,T_c) \equiv \int_0^\infty k(t,T_c)e^{-t/T_2}dt$ can be thought of as the "Laplace"-like transform of $k(t,T_c)$ and where we used the definition of $M(t)$ in eqn. (1).

The parameter T_c is user-specified and may come from laboratory study of rock and fluid properties or may correspond to a value of T_2 expected to separate two fluids in the T_2 domain [3].

The integral transform to compute tapered and sharp transitions ideally should satisfy the following properties: 1) the kernel $k(t,T_c)$ should exist $\forall t$ and $K(T_2,T_c)$ should exist $\forall T_2$, 2) based on the underlying petrophysics, it is desirable that $K(T_2,T_c)$ be monotonic between 0 and 1 with $\lim_{T_2\to 0} K(T_2,T_c) = 0$, $\lim_{T_2\to\infty} K(T_2,T_c) = 1$ and $K(T_2,T_c)\Big|_{T_2=T_c} = 0.5$, and 3) it should be possible to adjust the slope m in the $\log(T_2)$ space of the transition region with

$$m \equiv \left.\frac{dK(T_2,T_c)}{d\log T_2}\right|_{T_2=T_c}. \tag{5}$$

When the kernel $k(t,T_c)$ satisfies the above properties, the uncertainty in area A due to the additive noise in the data is

$$\sigma_A^2 = \sigma_\epsilon^2 t_E E \tag{6}$$

where σ_ϵ denotes the standard deviation of the additive noise in eqn. (1) and t_E is the sampling rate. The parameter E can be thought of as the "energy" of the function $k(t,T_c)$,

$$E = \int_0^\infty k^2(t,T_c)dt. \tag{7}$$

In general, we find that when $k(t,T_c)$ is square integrable with finite E, it gives rise to tapered areas in $\log(T_2)$ domain. Sharper transitions in the $\log(T_2)$ domain require larger E, resulting in larger uncertainty in the estimated area.

Next we describe a few simple integral transforms that provide tapered transitions, their properties and some practical experimental considerations that may help choose one transform over another. These transforms are also summarized in Table 1.

Sinc transform: The Laplace transform of a sinc function

with $k(t,T_c) = \frac{2}{\pi t}\sin\left(\frac{t}{T_c}\right)$ has a Heaviside-like behavior given by

$$K(T_2,T_c) = \frac{2}{\pi}\tan^{-1}\left(\frac{T_2}{T_c}\right) \quad (8)$$

where the complex frequency s of the Laplace transform has been evaluated at $1/T_2$. Its slope in the $\log(T_2)$ domain is the constant $m = 0.32$, according to eqn. (5).

Fig. 2 shows the sinc function and its corresponding Laplace transforms. The slope in the T_2 domain cannot be increased. However, it can be decreased by considering exponentially decaying functions multiplying the sinc function. From eqn. (7), the energy of the sinc function is $E = \frac{2}{\pi Tc}$. Thus, using eqn. (6), the uncertainty in the estimated area decreases with increasing T_c. This decrease in uncertainty in estimated area with increasing T_c underlines an important concept: the information regarding short relaxation times is only in the early echo data. Consequently, the amplitudes corresponding to early relaxation times have a larger uncertainty than those corresponding to the later relaxation times. This observation is consistent with the uncertainty estimates observed in [9].

Exponential Haar transform (EHT): Consider an exponentially decaying square wave of the form,

$$k(t,T_c) = A(-1)^n e^{-\beta t},\ 2n\alpha < t < 2(n+1)\alpha. \quad (9)$$

This function is a square wave whose amplitude is decaying exponentially. From analogy with the square-waves of the Haar wavelet transform, we refer to eqn. (9) as the exponential Haar transform.

Given an energy E, variables A, α and β can be determined to satisfy some of the properties enumerated earlier. For example, to have the same energy as the sinc function, we get $\alpha = (1.572)T_c$, $A = \frac{0.7213}{T_c}$ and $\beta = \frac{0.4087}{T_c}$. In this case, the slope in the $\log(T_2)$ domain is found to be $m = 0.35$,

Exponential Sine Transform (EST): Consider the exponentially decaying sine function $k(t,T_c) = \frac{\alpha^2+\beta^2}{\alpha^2}e^{-\beta t}\sin(\alpha t)$ where $\alpha = \sqrt{4E\beta - \beta^2}$ and $\beta = \frac{1}{T_c^2\left(4E - \frac{2}{T_c}\right)}$. Its corresponding Laplace transform is $K(T_2,T_c) = \frac{\alpha^2+\beta^2}{\alpha^2+\left(\beta+\frac{1}{T_2}\right)^2}$. The slope is m=0.3 and the energy is $E = \frac{2}{\pi T_c}$.

Fig. 2 shows the sinc transform, EHT and EST at T_c = 0.1. There is a practical consideration to prefer the EHT or EST to the sinc transform. The support in the time-domain of the EHT or EST kernels are smaller than that of the sinc function. Since field-log data are sometimes abruptly truncated in time (resulting in loss of information at large time), the sinc function which has a large support in the time domain is more likely to be biased when applied to measured field data. Table 1 summarizes the results.

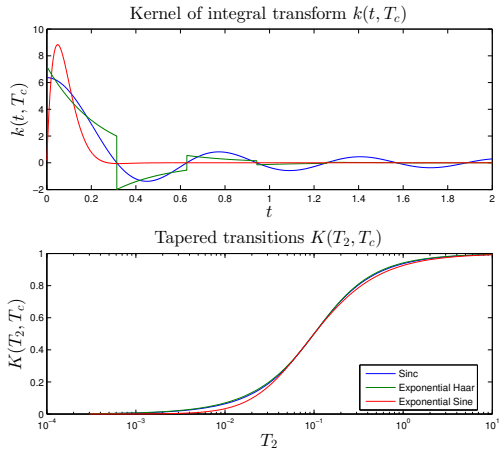

Fig. 2. Kernel of integral transforms for the calculation of tapered areas. Also shown are the corresponding tapered transitions.

3.1. Sharp Transitions

There are several ways to obtain sharper transitions. We can numerically construct $k(t,T_c)$ by essentially following a filter-design approach where using the truncated singular value decomposition of the forward mapping we can find approximate solutions. Another approach is based on the truncated Mellin transform applied to the derivative of the magnetization decay. It is possible to show that the linear transform $\frac{1}{\Gamma(\nu)}\int_0^T t^{\nu-1}\frac{d^\nu M}{dt^\nu}dt$ provides areas with a degree of sharpness given by ν. Finally a third approach is based on successive approximations where the kernel $k(t,T_c)$ of the integral transform is obtained from the inverse Laplace transform of $K_n(T_2,T_c) = g_0\left(\frac{T_c}{T_2}\right) + \sum_{k=1}^n a_k g_n\left(\frac{T_c}{T_2}\right)$ where g_n is a well chosen function that approximates the Heaviside function.

These methods will be described in a later communication.

4. SIMULATION RESULTS

In this sub-section we evaluate and compare the computation of area using EHT in the time-domain with the T_2 domain procedure of first computing $f_{T_2}(T_2)$ (ILT).

Noiseless data are simulated from the four T_2 distributions shown in Fig. 3 and corrupted with additive zero-mean, white, Gaussian noise with standard deviation $\sigma_\epsilon = 0.2$, simulating noisy data often present in field-logs. 100 noise realizations were simulated for each model. For all cases the sampling rate was $t_E = 200\mu s$. The number of samples was chosen so that the magnetization $M(t)$ decays to a small number.

Transform	Parameters	$k(t, T_c)$	$K(T_2, T_c)$	E	m
Sinc	$\alpha = \frac{1}{T_c}$	$\frac{2}{\pi}\frac{sin(\alpha t)}{t}$	$\frac{2}{\pi}\tan^{-1}(\alpha T_2)$	$\frac{2}{\pi T_c}$	0.32
Exponential	$A = \frac{0.7213}{T_c}$	$A(-1)^n e^{-\beta t}$	$\frac{A}{\left(\frac{1}{T_2}+\beta\right)}\tanh\left[\alpha\left(\frac{1}{T_2}+\beta\right)\right]$	$\frac{2}{\pi T_c}$	0.35
Haar	$\alpha = (1.572)T_c$				
	$\beta = \frac{0.4087}{T_c}$	$2n\alpha < t < 2(n+1)\alpha$			
Exponential	$\alpha = \sqrt{4E\beta - \beta^2}$	$\frac{\alpha^2+\beta^2}{\alpha}e^{-\beta t}sin(\alpha t)$	$\frac{\alpha^2+\beta^2}{\alpha^2+\left(\beta+\frac{1}{T_2}\right)^2}$	$\frac{2}{\pi T_c}$	0.3
Sine	$\beta = \frac{1}{T_c^2\left(4E-\frac{2}{T_c}\right)}$				

Table 1. Simple integral transforms that give rise to tapered transitions in the $\log(T_2)$ domain.

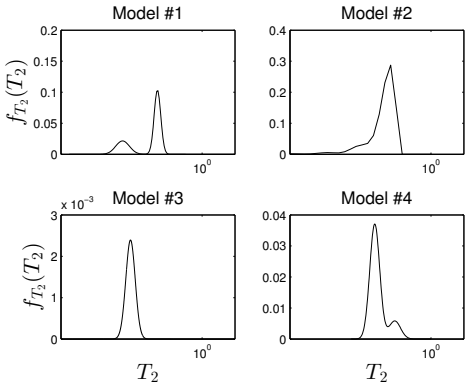

Fig. 3. Simulation models used for benchmarking.

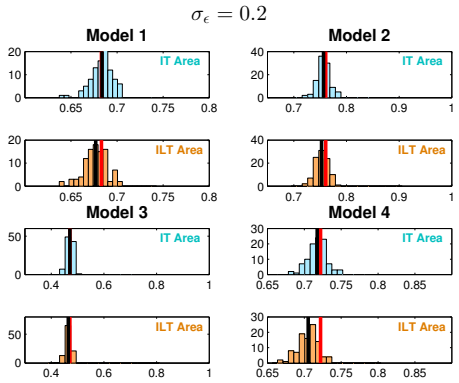

Fig. 4. Histograms of estimated tapered areas using inverse Laplace transform and integral transform.

The workflow used to compare the time-domain and T_2 domain methods is as follows. The noisy magnetization data $M(t)$ given in eqn. (1) and a specified T_c are inputs to both methods. The T_c values were chosen to be 33 ms. In the time-domain, the area from the EHT is computed in a straightforward manner using eqn. (9). In the T_2 domain, the T_2 distribution was obtained according to the Butler-Reeds-Dawson [10] which automatically selects the level of regularization according to the SNR. Next, the area A was computed using eqn. (4) with $K(T_2, T_c)$ corresponding to the exponential Haar transform.

The two methods are compared with respect to the normalized root mean square error computed in reference to the true value of A according to $nrmse = \frac{\sqrt{\langle(\hat{A}-A)^2\rangle}}{A} \times 100$.

The results of the analysis on 100 noisy data sets from each model are summarized in the histograms in Fig. 4. The bias in A is the difference between the mean (black line) and true value (red line) indicated in the figure. It is clearly seen, as expected, that the bias is larger when the computation is performed in the T_2 domain. The standard deviation of A from each method is also indicated in the figure by the spread of the points. Using eqn. (6), the expected standard deviation of A for each model is 0.0124 which matches the estimated standard deviation quite well as shown in Table 2.

Model	True	Area IT		Area ILT	
		$\mu \pm \sigma$	nrmse (%)	$\mu \pm \sigma$	nrmse (%)
1	0.683	0.684 ± 0.0116	1.69	0.677 ± 0.0126	2.05
2	0.761	0.756 ± 0.0126	1.74	0.753 ± 0.0124	1.93
3	0.471	0.471 ± 0.0112	2.38	0.465 ± 0.0116	2.79
4	0.722	0.717 ± 0.0127	1.87	0.705 ± 0.0141	3.03

Table 2. Mean, standard deviation, and normalized root means square error (nrmse) in the estimation of the tapered areas using the exponential Haar transform.

5. CONCLUSIONS

In this work we proposed alternative techniques for estimating tapered areas of the T_2 distribution directly from the measured magnetization decay in NMR experiments. This avoids the need to first solve the ill-conditioned problem of finding the T_2 distribution and has the additional advantage of given uncertainty estimates. We illustrated the performance on simulated experiments and showed that the parameters estimated by this new technique are better in terms of bias and standard deviation than the ones obtained by means of the traditional approach.

6. REFERENCES

[1] R. L. Kleinberg, C. Straley, W. E. Kenyon, R. Akkurt, and S. A. Farooqui, "Nuclear magnetic resonance of rocks: T_1 vs. T_2," *SPE*, vol. 26470, pp. 553–563, 1993.

[2] R. L. Kleinberg and A. Boyd, "Tapered cutoffs for magnetic resonance bound water volume," in *SPE Annual Technical Conference and Exhibition*, San Antonio, Texas, 5-8 October 1997, Society of Petroleum Engineers.

[3] C. Straley, D. Rossini, H. Vinegar, P. Tutunjian, and C. Morriss, "Core analysis by low-field NMR," *The Log Analyst*, vol. 38, no. 2, pp. 84–94, 1997.

[4] L. Venkataramanan, Y.-Q. Song, and M. D. Hürlimann, "Solving Fredholm integrals of the first kind with tensor product structure in 2 and 2.5 dimensions," *IEEE Transactions on Signal Processing*, vol. 50, pp. 1017–1026, 2002.

[5] J. G. McWhirter and E. R. Pike, "On the numerical inversion of the Laplace transform and similar Fredholm integrals of the first kind," *J. Phys. A: Math. Gen.*, vol. 11, pp. 1729–1745, 1978.

[6] C. L. Epstein and J. Schotland, "The bad truth about Laplace's transform," *SIAM Review*, vol. 50, pp. 504–520, 2008.

[7] N.J. Heaton, C. Cao Minh, J. Kovats, and U. Guru, "Saturation and viscosity from multidimensional nuclear magnetic resonance logging," in *SPE Annual Technical Conference and Exhibition*, Houston, Texas, September 2004, Society of Petroleum Engineers.

[8] L. Venkataramanan, F. K. Gruber, T. M. Habashy, and D. E. Freed, "Mellin transform of CPMG data," *Journal of Magnetic Resonance*, vol. 206, pp. 20–31, 2010.

[9] M. Prange and Y.-Q. Song, "Quantifying uncertainty in NMR T_2 spectra using Monte Carlo inversion," *Journal of Magnetic Resonance*, vol. 196, pp. 54–60, 2009.

[10] J. P. Butler, J. A. Reeds, and S. V. Dawson, "Estimating solutions of the first kind integral equations with nonnegative constraints and optimal smoothing," *SIAM J. Numerical Analysis*, vol. 18, no. 3, pp. 381–397, 1981.